Surface-Induced Near-Field Scaling in the Knudsen Layer of a Rarefied Gas

R. R. Gazizulin, O. Maillet, X. Zhou, A. Maldonado Cid, O. Bourgeois, and E. Collin
Université Grenoble Alpes, Institut Néel CNRS, 25 rue des Martyrs, BP 166, 38042 Grenoble Cedex 9, France

(Received 21 August 2017; published 19 January 2018)

We report on experiments performed *within* the Knudsen boundary layer of a low-pressure gas. The noninvasive probe we use is a suspended nanoelectromechanical string, which interacts with ^{4}He gas at cryogenic temperatures. When the pressure P is decreased, a reduction of the damping force below molecular friction $\propto P$ had been first reported in Phys. Rev. Lett. **113**, 136101 (2014) and never reproduced since. We demonstrate that this effect is independent of geometry, but dependent on temperature. Within the framework of kinetic theory, this reduction is interpreted as a *rarefaction phenomenon*, carried through the boundary layer by a deviation from the usual Maxwell-Boltzmann equilibrium distribution induced by surface scattering. Adsorbed atoms are shown to play a key role in the process, which explains why room temperature data fail to reproduce it.

DOI: 10.1103/PhysRevLett.120.036802

A low density gas is statistically described by the well-known Boltzmann kinetic theory [1–3]. The equilibrium state in the bulk, that is the distribution function f characterizing the molecular motion that cancels the collision integral $Q(f,f)$, is simply the well-known Maxwell-Boltzmann (MB) distribution f_0.

In any physical situation this equilibrium is imposed by *boundary conditions*: the gas is at temperature T_0, and pressure P_0 enforced by, e.g., the walls of a container. The interaction between gas particles and the solid surface is thus crucial, even in such a simple situation; in more complex cases where for instance a gas flow is forced near the wall, the presence of the interface generates unique features like slippage and temperature jumps [1,4–7]. All of this happens in a layer of thickness a few mean free paths λ, the so-called Knudsen boundary layer.

These features are essential in aeronautics and in the expanding field of micro- or nanofluidics [6,8,9], but their accurate modeling remains a challenge, even using today's numerical computational capabilities [10–13]. Already in the early days of the kinetic theory development, Maxwell had noticed the importance and difficulty represented by the boundary problem [14]; his discussion of molecular reflections (introducing an accommodation parameter p) is still valuable today.

The problem is indeed nontrivial, since the scattering mechanism on the wall depends intimately on details of complex surface physics phenomena like adsorption and evaporation of molecules. Besides, this introduces a strong asymmetry between incoming particles reaching the wall with the statistical characteristics of the gas, while escaping particles carry properties defined by the solid body [1,4,5,10,11].

In the present Letter we report on measurements performed within the boundary layer by means of a high quality nanoelectromechanical string (NEMS) device. We use ^{4}He gas at cryogenic temperatures, which is an almost-ideal gas with tabulated properties [15]. When the pressure P is sufficiently low, such that the mean free path of atoms is sufficiently long, we measure a decrease of the gas damping below the well-known molecular law $\Delta f_{\mathrm{molec}} \propto P$. Comparing different devices and measurements performed at different temperatures, we show that this anomalous decrease is consistent with a reduced gas density within the boundary layer. We can justify it as a deviation from the standard Maxwell-Boltmzann equilibrium distribution induced by the presence of the wall and its adsorbed atoms: a near-field effect propagated from the actual boundary scattering mechanisms that decays within the gas over a few mean free paths λ.

In Fig. 1 we show a schematic of the setup and a scanning electron micrograph (SEM) of the device. It consists of a high-stress silicon-nitride NEMS beam of $L = 150\ \mu$m length, width $w = 300$ nm and thickness $e = 100$ nm. A 30 nm thick aluminum layer has been deposited on top for electrical contacts [16]. The moving structure is suspended at a distance $g = 20\ \mu$m above the bottom of the etched chip. Its motion is actuated and detected through the magnetomotive scheme [17,18]: a current $I_0 \cos(\omega t)$ oscillating at frequency ω close to the first out-of-plane flexure resonance ω_0 is fed in the metallic layer while the structure resides in an in-plane magnetic field B_0 orthogonal to the beam. The resulting Lorentz force F_0 generates the motion while the voltage induced by the cut magnetic flux V_0 is detected by means of a Stanford© SR844 lock-in amplifier. Details on the scheme and calibration can be found in Ref. [18] and the Supplemental Material [19].

The device is glued on a copper plate, which is mounted in a chamber placed inside a ^{4}He cryostat. The pressure is

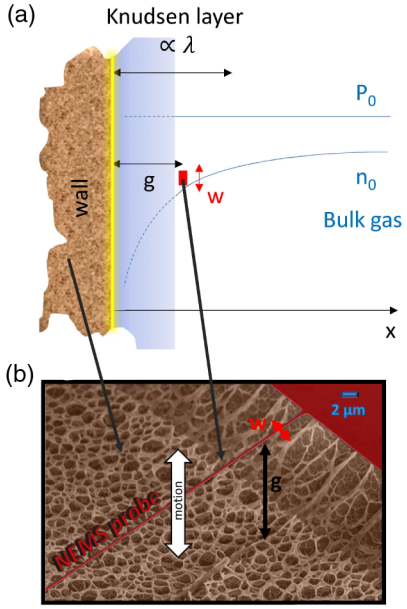

FIG. 1. (a) Schematic of the experimental situation with in brown the container's surface (on left), in light yellow the adsorbed atoms and then the gas (bulk on the far right). The pressure P_0 remains constant while the density $n(x)$ drops from n_0 as we approach the wall, within a thickness of order a few mean free paths λ (Knudsen layer). Our NEMS local probe of width w lies a distance g from the surface (red rectangle). Close to the wall, macroscopic theories based on simple expansions fail to describe the physics, and delicate microscopic modeling or numerical simulations are required (shaded area). (b) Actual device used in this work (SEM false color image), in which oscillatory motion is orthogonal to the wall (arrow). Note the spongy nature of the interface.

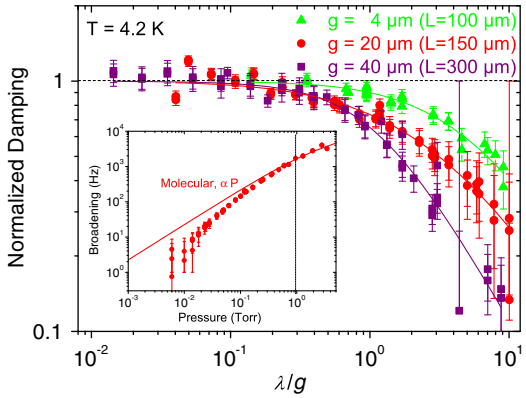

FIG. 2. Main: Deviation form molecular damping (proportional to P) measured at low pressures, for three devices at 4.2 K as a function of the Knudsen number λ/g. The lines are fits to Eq. (1), see text. Inset: Raw data for the 150 μm long device (intrinsic damping subtracted); the full line is the standard molecular damping expression, and the vertical dashed line shows the crossover to Navier-Stokes damping (see text).

measured at room temperature using a Baratron© pressure gauge. ^{4}He gas was added by small portions to the cell from the evaporation of a dewar connected through a needle valve. The temperature is lowered from 4.2 K down to 1.3 K by pumping on the ^{4}He bath of the cryostat. It is regulated up to 20 K by means of a heater attached to the copper sample holder. The temperature is measured from the other side with a calibrated carbon resistor connected to a bridge. More details can be found in the Supplemental Material [19].

We first perform measurements at 4.2 K as a function of pressure. Subtracting the intrinsic damping of the mode (about 100 Hz), we plot in the Fig. 2 inset the broadening Δf of the resonance as a function of P. The drive has been kept low enough to be in the linear regime, and the resonance is a Lorentzian peaked around 1.65 MHz. No particular nonlinear damping has been noticed in the measurements. When the pressure remains below typically 1 Torr, the gas is said to be in the molecular regime: the mean free path is long and the gas damping on the NEMS device has to be described by molecular shocks transferring momentum [20,21]. At higher pressure, the fluid can be described by the Navier-Stokes equations [22]. The crossover between the two regimes is a complex issue that has attracted interest recently for both fundamental and practical reasons [23,24]. Besides controlling thermal gradients in the cell and NEMS velocities, we believe that there is no relevant net (static or oscillatory) flow around the boundary in our experiments (see Supplemental Material [19]).

When the pressure is low enough such that the mean free path λ is of the order of the gap g, we observe a reduction of the damping below the expected $\Delta f_{\mathrm{molec}} \propto P$ molecular law (Fig. 2 inset). This was first reported in Ref. [25] for two other devices of different length L and gap g. However, at that time, the low-pressure analytic interpretation was not specific and a tentative power-law fit had been proposed. In the main graph of Fig. 2 we plot the broadening normalized to the standard molecular law $\Delta f/\Delta f_{\mathrm{molec}}$ with respect to λ/g, the relevant Knudsen number in our problem. These data are compared with that of the two devices of Ref. [25], analyzed in the same way. By construction all curves start at 1, and decrease for larger λ/g with up to a factor of 10 reduction in damping, which is remarkable.

The shape of the measured curves in Fig. 2 for different devices is rather similar; assuming that indeed the analytic dependences should be the same, we show that all data can be fit consistently by the same Padé approximant leading to the same asymptotic laws:

$$\frac{\Delta f}{\Delta f_{\mathrm{molec}}} = \frac{1 + c\frac{\lambda}{g}}{1 + (c-\alpha)\frac{\lambda}{g} + \frac{c}{\alpha'}\left(\frac{\lambda}{g}\right)^2}, \qquad (1)$$

which gives $1 + \alpha(\lambda/g)$ at first order ($P \approx 1$ Torr) and $\alpha'(g/\lambda)$ when the pressure is very low $P \ll 1$ Torr. The parameter c then captures the rounded shape that joins these two limits in Fig. 2 (see Supplemental Material [19] for details).

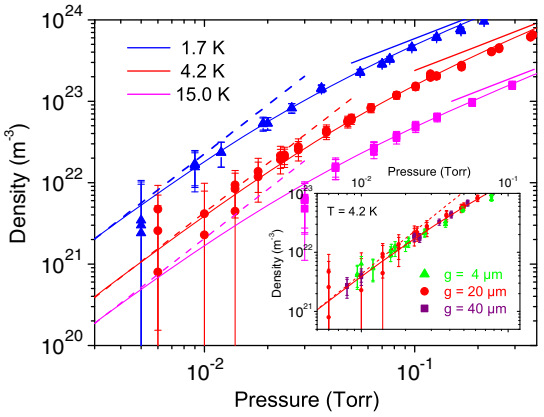

FIG. 3. Main: Effective density calculated at three different temperatures for the 150 μm long device. Thin lines correspond to fits obtained from Eq. (1) while the thick lines at high pressure ($\propto P$) and the dashed lines at low pressures ($\propto P^2$) are the asymptotes. Inset: Same data at 4.2 K for the three different devices, showing the independence towards g.

Remarkably, the parameter α is independent of the gap g, which proves that indeed the crossover from the standard molecular regime to the boundary layer regime occurs when $\lambda \approx g$. However, α' is inversely proportional to g meaning that when the NEMS device is deeply immersed into the boundary layer, the measured gas damping is *independent* of g (Fig. 3 inset). This is also to be expected, since in this limit $\lambda \gg g$ and g cannot be a relevant length scale anymore: essentially the local probe senses molecular shocks *almost on* the boundary surface.

The first order deviation $\alpha(\lambda/g)$ to molecular scattering can be accounted for by adapting known kinetic theory models. The idea is that the boundary scattering on the surface induces deviations from the MB equilibrium distribution that propagate within the gas over a length scale commensurate with the mean free path. Furthermore, we shall demonstrate that the mathematical development interprets the measurements as a *rarefaction phenomenon* occurring within the boundary layer: locally, because of the deviations to MB distribution the gas density is reduced.

The starting point consists in noting that the NEMS probe is essentially a noninvasive sensor since $w \ll \lambda$ and $w \ll g$ [25]. As such, all deviations to standard molecular damping have to proceed from the boundary scattering. On the wall, the collision integral $Q_{\text{wall}}(f,f)$ writes formally as follows:

$$Q_{\text{wall}}(f,f) = \int\int (f'f_1' - ff_1)B[\Omega, \vec{v}, \vec{v}_1]d\Omega d\vec{v}_1, \qquad (2)$$

with $B(\Omega, \vec{v}, \vec{v}_1)$ the scattering kernel produced by the actual interaction on the surface, the notations corresponding to the process $\{\vec{v}, \vec{v}_1\} \rightarrow \{\vec{v}', \vec{v}_1'\}$ [1]. The distribution function $f(\vec{v})$ verifies the Boltzmann equation, but on the wall there is *no reason* for the complex interactions between gas particles and adsorbed atoms to zero the collision integral, leading to $Q_{\text{wall}}(f,f) \neq 0$.

This implies [1] that $f \neq f_0$ (the MB distribution) close to the surface, and we assume the deviation to be small and regular enough to be expanded in powers of the particles' velocity field $\vec{v}$:

$$f(\vec{v}) = f_0(1 + Pl[\vec{v}]), \qquad (3)$$

with $Pl(\vec{v})$ a polynomial. This is essentially the approach first proposed by Grad [1–5], but we do not assume here any particular polynomial form since we do not know the symmetries of the scattering kernel B. We proceed by applying the Chapman-Enskog method to the coefficients of the polynomial Pl themselves [1,2]: we assume that *each of them* can be developed in a series of λ/x.

The combination of the two mathematical techniques (Grad and Chapman-Enskog) does not aim at calculating these parameters; it is essentially a phenomenological macroscopic approach which enables us to justify the analytic form Eq. (1) in its "high pressure" asymptotic dependence (the $P \approx 1$ Torr range, when $(\lambda/g) \approx 1$). The interesting aspect of the mathematical treatment lies in the fact that we do not need to stipulate the scattering kernel B. Furthermore, it is not a trivial expansion: the calculation has been performed up to order 4 in velocity, and order 3 in Knudsen number in order to demonstrate that indeed the approach is self-consistent. As a result, one obtains the macroscopic thermodynamical parameters temperature $T(x) = T_0 + \delta T(x)$, density $n(x) = n_0 + \delta n(x)$, and kinetic pressure along the $\vec{x}$ axis $P_{xx}(x) = P_0 + \delta P(x)$ as Taylor series in λ/x depending on the near-field parameters introduced by the expansions.

The key result is that the kinetic pressure $P_{xx}(x)$ is constant within the boundary layer ($\delta P[x] = 0$), the temperature contains a second order correction at lowest order $\delta T(x) \propto (\lambda/x)^2$ leading to the known temperature jump phenomenon on the surface [26], while the density deviation is first order $\delta n(x) \propto (\lambda/x)$. This is schematized in Fig. 1(a), with the device probing the $x = g$ position in space: in this sense, the measured first order *decrease* of the friction force with respect to molecular damping is due to the rarefaction of the gas in the boundary layer. Details on the calculation can be found in Supplemental Material [19].

This macroscopic approach is robust, provided all the expansions are defined. These hypotheses essentially mean that we consider the mathematical treatment far enough from the surface ($x = 0$ is indeed pathological). What happens very close to the surface is an extremely complex problem as far as mathematics are concerned, far beyond the phenomenological approach. Note also that in the literature, the deviations from MB distribution close to a wall are discussed usually in the framework of gas flows [1,4,10–12]; here, the complex nature of the interaction with the surface is the only source of deviations. The gas is at equilibrium, with a continuous dynamic exchange of atoms between the adsorbed ones and the gas boundary, but the

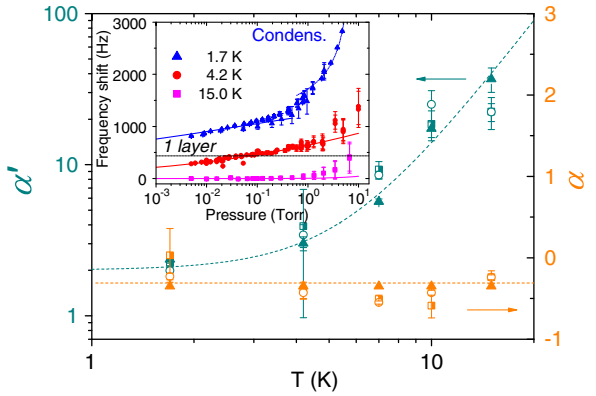

FIG. 4. Main: Leading-order coefficients extracted from the fits of Fig. 2. Different symbols stand for different fitting routines (see Supplemental Material [19]). Dashed lines are guides for the eye. Inset: Measured frequency shifts due to adsorbed layers onto the NEMS surface for three temperatures. For 1.7 K and 4.2 K, data obtained on the different devices have been normalized to the $L = 150$ μm one [19]. At 1.7 K, the rapid growth when P is increased corresponds to the condensation of a thin superfluid film [19,27,28], while at higher temperatures the weaker growth is a signature of the crossover towards the Navier-Stokes regime. Lines at low pressures are fits based on Dubinin-Astakhov isotherms [19,29–32], while the horizontal dashes correspond to a *dense* adsorbed monolayer [33].

distribution of velocities is non-MB: the spatial gradients can be seen as due to a near-field force which originates on the boundary, from the presence of the adsorbed atoms.

By changing temperature T we can also tune the mean free path λ [19]. Besides, since the decrease in damping is essentially due to a decrease in density, we can compute an effective density $n_{\mathrm{eff}} \equiv n$ in the boundary layer from the molecular damping expression $\Delta f_{\mathrm{molec}} \propto n$. We present in Fig. 3 these measurements with the $L = 150$ μm NEMS device at three different temperatures. We see that the data can again be very well fit by the Padé approximant Eq. (1). At high pressures, we find, as we should, the asymptotic deviation $\alpha(\lambda/g)$ for the effective density. Remarkably, the fit coefficient α appears to be also temperature independent; this is shown in Fig. 4.

On the other hand, at low pressures the effective density scales as P^2 (dashed lines in Fig. 3). This corresponds to the $\alpha'(g/\lambda)$ asymptotic behavior already discussed when we introduced Eq. (1). In the inset of Fig. 3 we show that the measured effective density does not depend on the gap g, as it should. The fit parameter α' is presented in Fig. 4; as opposed to α, it strongly depends on temperature.

The fact that α is temperature independent suggests that the first order deviation is essentially driven by the physical mismatch that the surface introduces in the problem, regardless of the *excitations* that it can support. In this sense, the first order deviation in Knudsen number λ/g seems to be *universal*. However, in the other limit, α' depends on temperature, and seems to increase rather quickly when the temperature becomes equivalent to the adsorption energy (Fig. 4). In the inset of Fig. 4, we show how the NEMS resonance frequency shifts when mass is added through adsorbed layers. Even if the NEMS surface is physically not the same as the probed boundary [the spongy background in Fig. 1(b)], this gives us important information about the surface coatings present in the experimental cell [19]; in particular, we can estimate the number of adsorbed atomic layers. The growth of α' correlated with the adsorption temperature proves that the surface coating plays an important role in the scattering mechanisms at very low pressures. Besides, it explains why the rarefaction effect could not be demonstrated at room temperature [34]; indeed in Fig. 3, as the temperature is increased the cusp in the measured friction (change from P^2 to P laws) becomes less and less visible.

In conclusion, we measured the friction force exerted by ^{4}He gas at cryogenic temperatures on a NEMS device. When the pressure is very low, we report on a decrease from the standard molecular damping $\Delta f_{\mathrm{molec}} \propto P$. We explain how this effect can be interpreted in terms of a *rarefaction* of the gas near the surface boundary, induced by a deviation from the standard Maxwell-Boltzmann equilibrium distribution. This phenomenon can be seen as a near-field force propagating within the gas over a length commensurate with the mean free path λ, the Knudsen layer. Deep in the boundary layer, the effective density of the gas seems to scale as P^2 instead of P. All the experimental data can be fit using a simple Padé approximant expression, demonstrating that the first order deviation from molecular damping is temperature and geometry independent. On the other hand, the P^2 dependence is also a function of temperature, strongly marked by the adsorption energy of ^{4}He atoms on the chip surface. This demonstrates the importance of the dynamics of adsorbed atoms in this effect, and explains why room temperature experiments fail to reproduce it. The phenomenon should be accompanied by a temperature jump, and is clearly calling for further theoretical and experimental developments.

We thank J.-F. Motte, S. Dufresnes, and T. Crozes from facility Nanofab for help in the device fabrication. We acknowledge support from the ANR Grant MajoranaPRO No. ANR-13-BS04-0009-01 and the ERC CoG Grant ULT-NEMS No. 647917. This work has been performed in the framework of the European Microkelvin Platform (EMP) collaboration.

[1] C. Cercignani, *Mathematical Methods in Kinetic Theory* (Springer Science and Business Media, New York, 1969).
[2] S. Chapman and T. G. Cowling, *The Mathematical Theory of Non-Uniform Gases*, 3rd ed. (Cambridge University Press, Cambridge, England, 1970).
[3] H. Grad, Commun. Pure Appl. Math. **2**, 331 (1949).

[4] G. N. Patterson, *Molecular Flow of Gases* (John Wiley & Sons Inc., New York, 1956).
[5] Y. Sone, *Molecular Gas Dynamics* (Birkhauser, Boston, 2007).
[6] J. Laurent, A. Drezet, H. Sellier, J. Chevrier, and S. Huant, Phys. Rev. Lett. **107**, 164501 (2011).
[7] D. A. Lockerby, J. M. Reese, D. R. Emerson, and R. W. Barber, Phys. Rev. E **70**, 017303 (2004).
[8] E. Gil-Santos, C. Baker, D. T. Nguyen, W. Hease, C. Gomez, A. Lemaitre, S. Ducci, G. Leo, and I. Favero, Nat. Nanotechnol. **10**, 810 (2015).
[9] L. Bocquet and J. L. Barrat, Soft Matter **3**, 685 (2007).
[10] S. Kokou Dadzie and J. Gilbert Méolans, Physica (Amsterdam) **358A**, 328 (2005).
[11] C. R. Lilley and J. E. Sader, Phys. Rev. E **76**, 026315 (2007).
[12] C. R Lilley and J. E Sader, Proc. R. Soc. A **464**, 2015 (2008).
[13] T. Wu and D. Zhang, Sci. Rep. **6**, 23629 (2016).
[14] J. C. Maxwell, Phil. Trans. R. Soc. London **170**, 231 (1879).
[15] V. D. Arp and R. D. McCarty, *Thermophysical Properties of Helium-4 from 0.8 to 1500 K with Pressures to 2000 MPa, NIST Technical Note No. 1334* (NIST, Boulder, Colorado, 1989).
[16] M. Defoort, K. J. Lulla, C. Blanc, H. Ftouni, O. Bourgeois, and E. Collin, J. Low Temp. Phys. **171**, 731 (2013).
[17] A. N. Cleland and M. L. Roukes, Sens. Actuators **72**, 256 (1999).
[18] E. Collin, M. Defoort, K. Lulla, T. Moutonet, J.-S. Heron, O. Bourgeois, Yu. M. Bunkov, and H. Godfrin, Rev. Sci. Instrum. **83**, 045005 (2012).
[19] See Supplemental Material at http://link.aps.org/supplemental/10.1103/PhysRevLett.120.036802 for details on the experimental setup and calibrations, and the mathematical treatment based on both the Grad and Chapman-Enskog methods.
[20] K. Yamamoto and K. Sera, Phys. Fluids **28**, 1286 (1985).
[21] R. B. Bhiladvala and Z. J. Wang, Phys. Rev. E **69**, 036307 (2004).
[22] J. E. Sader, J. Appl. Phys. **84**, 64 (1998).
[23] V. Kara, V. Yakhot, and K. L. Ekinci, Phys. Rev. Lett. **118**, 074505 (2017).
[24] E. C. Bullard, J. Li, C. R. Lilley, P. Mulvaney, M. L. Roukes, and J. E. Sader, Phys. Rev. Lett. **112**, 015501 (2014).
[25] M. Defoort, K. J. Lulla, T. Crozes, O. Maillet, O. Bourgeois, and E. Collin, Phys. Rev. Lett. **113**, 136101 (2014).
[26] C. E. Siewert, Phys. Fluids **15**, 1696 (2003).
[27] J. G. Dash, *Films on Solid Surfaces* (Academic Press, London, 1975).
[28] F. Pobell, *Matter and Methods at Low Temperatures* (Springer, New York, 1996).
[29] M. M. Dubinin and V. A. Astakhov, Izv. Akad. Nauk USSR, Ser. Khim. **1**, 5 (1971) [Bull. Acad. Sci. USSR **20**, 3 (1971)].
[30] W. Rudzinski and D. H. Everett, *Adsorption of Gases on Heterogeneous Surfaces* (Academic Press, London, 1992).
[31] G. F. Cerofolini, Surf. Sci. **24**, 391 (1971).
[32] N. D. Hutson and R. T. Yang, Adsorption **3**, 189 (1997).
[33] P. H. Schildberg, Ph.D. thesis, Institut Laue Langevin, 1988; reprinted in H. Godfrin and R. E. Rapp, Adv. Phys. **44**, 113 (1995).
[34] V. Kara, Y.-I. Sohn, H. Atikian, V. Yakhot, M. Loncar, and K. L. Ekinci, Nano Lett. **15**, 8070 (2015).